National Conference with International Participation
ENGINEERING MECHANICS 2007
Svratka, Czech Republic, May 14 – 17, 2007

High-speed droplet impact during hydraulic descaling process

A. Horák*, J. Boháček*

Summary: *The steel hot rolling process is inseparably connected to the oxidation of a rolled material at increased temperatures. Hydraulic descaling of rolled material is a part of all rolling trains. Surface quality after descaling is fundamental for the total surface quality of a roll product. The process itself is not theoretically well described; various different approaches were used to clarify the descaling problem. This paper describes the dynamics of high-speed impact between compressible water droplet and steel scale layer. The purpose of this study is to verify the fact that impact stress can be a significant factor during descaling process. Considering high droplet impact speed (100-300 ms^{-1}), inferential extremely short time intervals (0.1-5.0 μs) and complicated scale structure model presents only qualitative illustration. This model uses the finite element method and applies boundary conditions based on water-hammer effect, needed for the evaluation of tensile stress in a layer of scales and in the basic steel material.*

1. Introduction

Descaling occurs through the application of energy or force by the descaling systems. There are several mechanisms suggested for the active mechanism of descaling. Two major approaches can be found in the literature “mechanical concept and thermal concept”.

The mechanical theory says that the force of the water applied to the steel is sufficient to pulverize the scale into small particles and thus remove it from the steel substrate. A similar water-impact concept is that the scale is removed by a mechanical force applied to its through-thickness face [1]. This theory leads to the conclusion that the oblique jet impact provides a better performance than the perpendicular impact. The tests of the surface quality after descaling were conducted at the Brno laboratory. The impact angles of 0°, 8°, 15°and 30°were applied. These tests do not show better results for a large inclination of the angles.

The thermal theory is mostly based on the thermal expansion mismatch between scale and steel that causes a large mechanical shear forces at the scale-steel interface during chilling. Thermal inducted force can reach two order of magnitude higher forces than the measured mechanical force applied by water [2].

* Ing. Aleš Horák, Ing. Jan Boháček, Laboratoř přenosu tepla a proudění, Fakulta strojního inženýrství, VUT Brno, Technická 2896/2, 616 69, Brno, tel.: + 541 143286, e-mail: bohacek@lptap.fme.vutbr.cz

Another mechanism is that of vapour explosion [3]. Water can infiltrate the cracks in the scale and evaporate almost instantly due to a high material temperature. The rapid evaporationcreates an instant increase in vapour pressure producing a high shear stress between scale and substrate or among the scale layers.

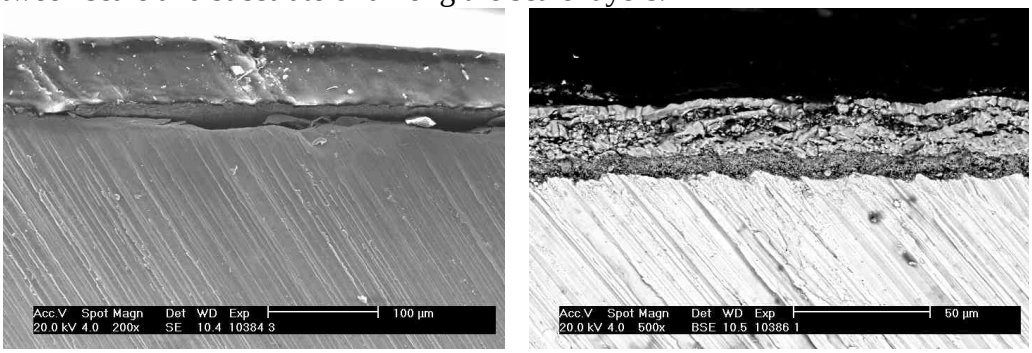

Fig.1: Electron microscope photo of steel-scale composition layer.

The descaling process can be also explained by the high-velocity impact of water drops or jets. The theory of a so-called Water-Hammer Effect says that high speed liquid-solid collision causes extremely height of stress within a solid body resulting in structure disintegration. This effect is known from e.g. cutting technology [4] and also it is experimentally studied at the n Heat Transfer and Fluid Flow Laboratory (Fig. 2). For understanding of this phenomenon, spatial and temporal pressure distribution acting on target surface must be known. With this knowledge used as boundary conditions, the transient stress within solid (both in steel and scale layer) can be calculated. The most important values to know are the pressure maximum and the moment when it occurs. There are different theories describing jet or droplet impacts. The most valuable are described below.

Considering a stable jet of ideal liquid (non compressible and non viscose), with perpendicular impact onto a rigid surface, the impact pressure p_s is equal to [5]:

$$p_s = \frac{1}{2}\rho v_0^2 \quad (1)$$

where ρ is the liquid density and v_0 is impact velocity. These assumptions oversimplify the problem too much and the liquid compressibility must be taken into account. In such a case the impact pressure for jet (2a) and for spherical droplet (2b) given by the water-hammer effect is given by [6]:

$$p_i = \rho v_0 c_0 \ , \quad (2a) \quad \text{and} \quad p_i = \frac{1}{2}\rho v_0 c_0 \ , \quad (2b)$$

where c_0 is the sonic velocity (1500 ms^{-1} for water). The mechanism of the water-hammer effect, shown in Fig 3 (on the left), is based on shock wave propagation. Impact shock wave propagation occurs with sonic velocity immediately after the impact and therefore a rapid initial pressure increase is observed. At the same time a relax wave arising from the edges to the middle of the jet starts to move. Maximum pressure p_i (2a) is reached after the relax wave arrives to the midpoint and time t_i at this moment is equal to:

$$t_i = \frac{r}{c_0} \quad (3)$$

where r is droplet radius. Considering water jet diameter (e.g. 1 mm), the ultimate process is extremely short and impact pressure maximum occurs at 0.33 μs. Since the relax wave arrives

into the drop/jet center impact pressure is decreasing from maximum p_i to steady state p_s and lateral jet-spreading begin.

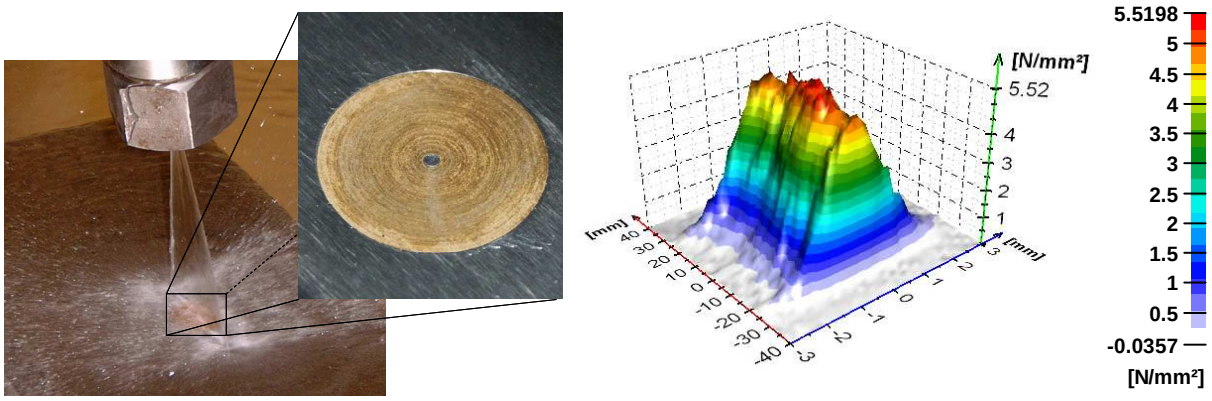

Fig.2: Detailed photo of the pressure sensor (left) and the typical measured pressure distribution for the descaling nozzle (right), with a feeding pressure of 200 Bars.

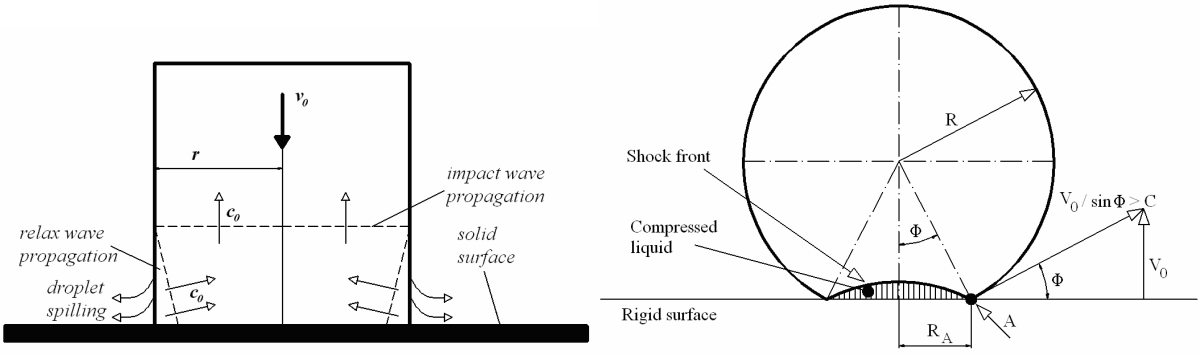

Fig.3: Water-hammer effect during water jet (left) and spherical droplet (right) impact.

In [7] Huang discovered a non-constant shock wave propagation velocity, which is in addition higher than sonic velocity $\boldsymbol{c_0}$ and depends on jet impact velocity $\boldsymbol{v_0}$. For water shock wave velocity is given by the following formula:

$$c = c_0 + 2v_0 - 0{,}1\frac{v_0^2}{c_0} \quad (4),$$

a maximum pressure value becomes equal to:

$$p_i = \rho v_0 c \quad (5).$$

A similar conclusion, presented by Heyman [8], where initial contact area is at one point, and then the contact area grows during the impact process, and is expressed by:

$$p_i = \rho v_0 c_0 [1 + k(\frac{v_0}{c_0})] \quad , \quad (6)$$

where k is a constant specific to each liquid. In [9] Heyman with analogical assumptions using a limiting contact angle Φ_c creates an impact model for a spherical droplet. The mechanism is the following: in the initial stages, during which liquid is entirely compressible and no lateral outflow occurs; the liquid-solid contact area is growing faster than shock wave propagation velocity. At this moment high pressure area inside droplet (Fig. 3 right) exists, which is bordered by a rigid surface and a shock wave front. When the shock wave overtakes

the interface perimeter lateral outflow occurs. The limiting contact angle at which shock front becomes detached is given by:

$$\sin \Phi_c = \frac{v_0}{c} \quad (7).$$

As long as contact angle do not reach approximately half of $\boldsymbol{\Phi_c}$ contact pressure is almost equal to 1-D model. Afterwards, the impact pressure grows with increasing velocity to a maximum culminating in the equation:

$$p_i = 3\rho v_0 c_0 \quad (8) \quad \text{, for impact velocities between } 0.03 < v_0/c < 0.3,$$

$$\text{and } p_i = \rho v_0 c_0 (2 + 3\frac{v_0}{c_0}) \text{ for higher impact velocities.} \quad (9)$$

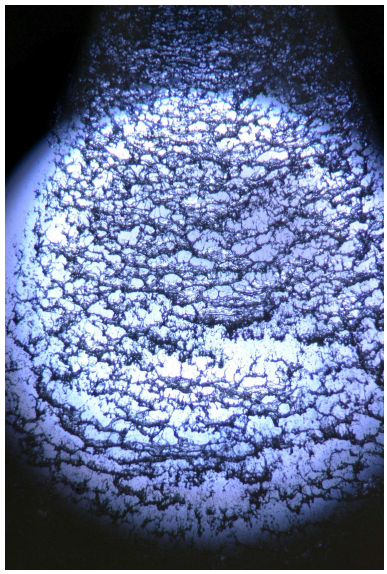

Fig.4: Short time photo of the spray fan from a descaling nozzle, feeding pressure 200 bar, distance from orifice 50 mm, image size 30x50 mm.

Although measured impact pressure is considered as a highly demanding research topic, particularly because of the extremely high pressure values measurable during a very short time period, several studies have been published. Bruton in [10] determines by experiment that average impact pressure values for a water jet (v_0=731.7 ms^{-1}; r =2.15 mm) reach 924 MPa (formula (2a) gives 1080 MPa) in a time interval of 1 µs (1.43 µs by formula (3)). In a time interval of 3 µs the impact pressure decreases to the steady state value p_s.

Smith & Kinslow present in [6] results for water jet front diameter of 6,6 mm and impact velocity of 640 ms^{-1}, where maximum the impact pressure on the impact area midpoint was observed as 863 MPa (p_i=945 MPa by formula (2)). Impact pressure maximum occurs at time interval 3 µs (formula (3) gives 2.2 µs) and after 5-6 µs, pressure decrease to steady state p_s.

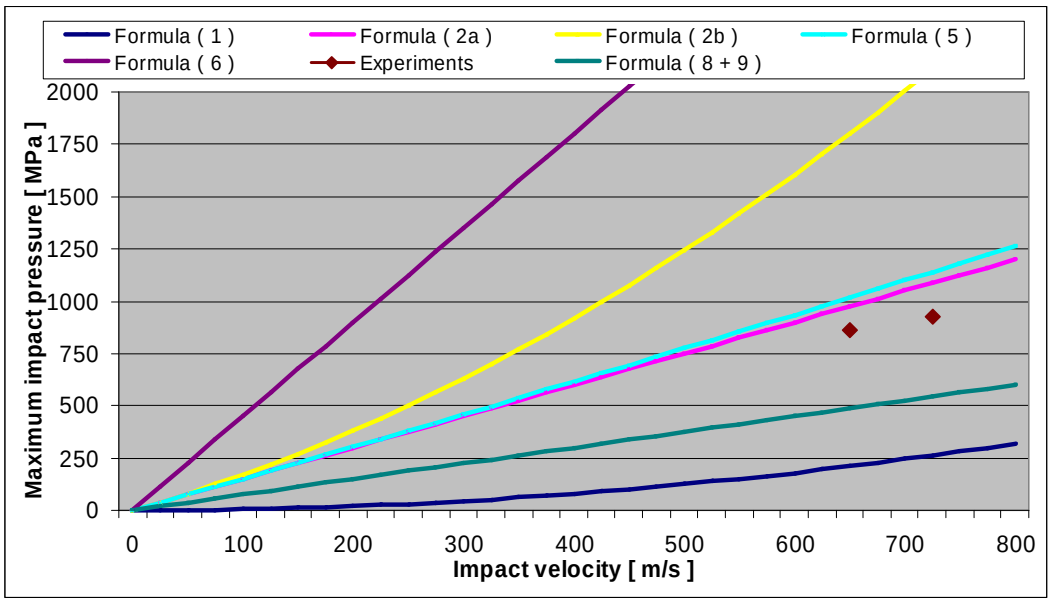

Fig.5: Impact pressure as function of impact velocity for different formulas.

All presented models and equations for maximum impact pressure are compared in Fig.5, where experimental data from [6] and [7] are also included. Previous data agrees with the aforementioned formulas [2a] and [5]. With regard to the accuracy of experiment data it is important to consider the size of the pressure sensor; high pressure during only a short time period must be taken in account, since it is otherwise not clear enough if the maximum or the average values were measured. Fig. 5 shows the differences among maximum pressures in the formulas (2a), (2b), (5), (6) and (8 + 9), which are several times higher than steady state pressure given by (1).

2. Numerical models

Maximum impact pressure values arising from the water-hammer theory are sufficient for breaking scale layer. In addition to our modelling and computation pressure history must be known as well. Numerical simulations of 2-dimensional droplet impingement were treated by Huang ([13], [18]) using mathematical model based on Compressible-Cell-and Marker Method (ComCAM). Considering a compressible non-viscose liquid, the solution for collision with a rigid plane surface was performed for cylindrical, spherical and cylindrical-spherical composite droplet. Shape of high-droplet geometry is as it is shown in Fig.4 very heterogeneous. Huang's results show a supposed scenario: huge pressure increased after initial collision from 0 to the maximum and the relaxation to steady state pressure in an expected time slot. These pressure distributions are used for design of boundary conditions into steel-scale layers stress analysis. The first step of this study must be the confirmation of the results presented in [13] and [18], especially, pressure time history and droplet impact disintegration. The impact pressure maximum and time have to be acknowledged to make sure that our boundary conditions based on literature [5-20] are correct. On contrast Huang, 3-dimensional model using LS-Dyna solver, the Finite Element Method (FEM) was used. This 3D model allows studying the droplet impact disintegration, pressure distribution within a single water droplet and time histories. Our analysis and computation focus on the single water droplet of 3 mm diameter, assuming a droplet impact velocity of 300 ms^{-1} and a total rigid surface.

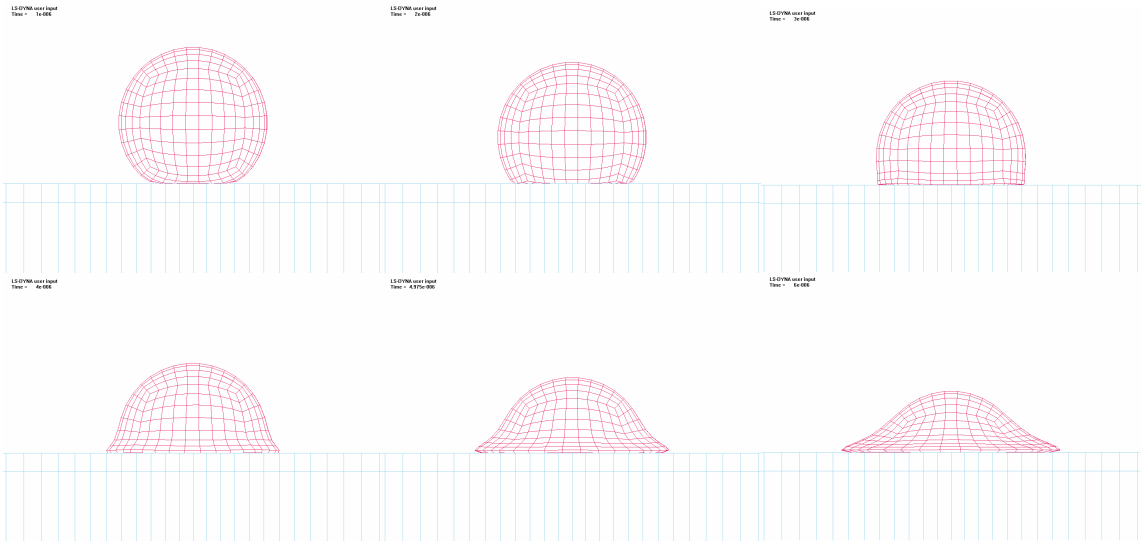

Fig.6: Single water droplet disintegration in time period: 1, 2, 3, 4, 5 and 6 µs; 300 ms^{-1} and 3 mm diameter, maximum pressure occurs in time interval 1-2 µs.

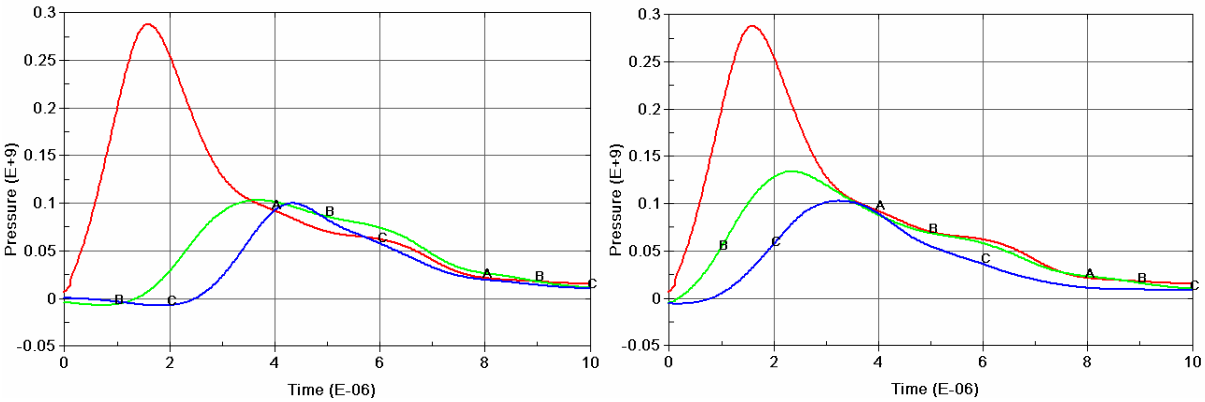

Fig.7: Pressure history within droplet along droplet diameter (left - red line (A) surface, green (B) ½ radius and blue (C) droplet centre) and along droplet surface (right - red line (A) axis of symmetry, green (B) 0.125 mm and blue (C) 0.25 mm from droplet axis).

3. 2D model with scale layer

The model presented in this paper focuses on stress modelling of a scale-steel body hit by a high-speed water drop. Settings of droplet velocity and a diameter value defines stress within scale-steel system and time duration of process. A uniform circular water jet distribution along **y** axis is assumed, which simplifies the model from solving 3-Dimension to 2-D task and makes the modelling much faster,. The Finite Element Method Model contains two layers of given thickness – scale layer (50 and 500 µm were simulated) and whole model (10 mm). For a superior understanding of the scale behavior (very heterogeneous structure) under the stress two models were performed (Fig. 8), model A with no crack and model B with 50 µm crack in the centre. Proper scale geometry, shown in Fig.1, is difficult to be set because of a very random structure. The model width is 5 mm and total simulated time is 10 µs. It is

important to know the material properties of steel and scale layer. Especially for the scales, considering heterogeneous structure, precise properties are hard to acquire. The presented model applies the properties of scales and carbon steel (0.4 % C), taken from [21]. The force distribution along time and x coordinates re-computed from droplet impact pressure (based on Huang's 2D and our 3D model) was used as boundary condition for the computation. Fig.8 (right) shows the typical pressure distribution – a rapid pressure increase up to the maximum during a very early/initial time period following by a pressure falling and propagation from the centre to the edges. Varying with boundary condition different parameters of liquid-solid collision can be simulated. The model was also solved by LS Dyna solver, which is an extension of the FEM solver ANSYS, used for dynamic simulations. For our purposes 2D elements method of type Plane 162 was chosen.

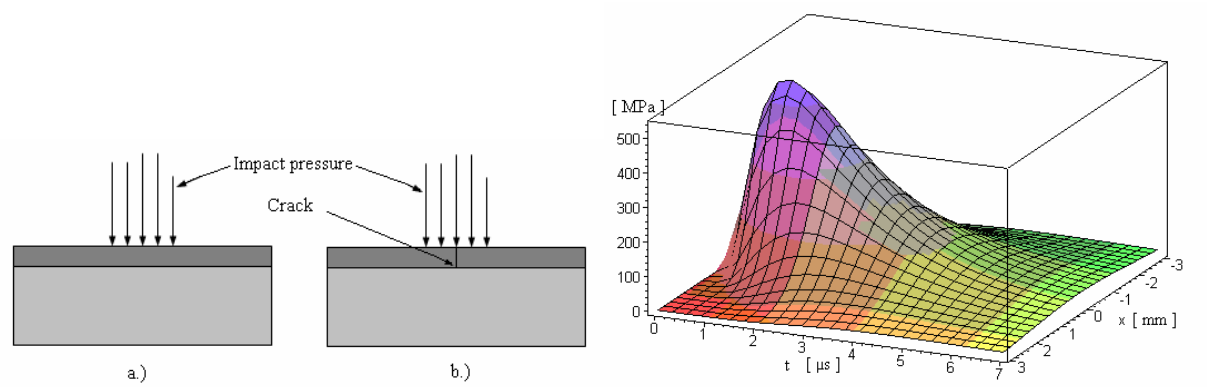

Fig.8: Impact pressure as boundary condition for model A (without crack) and B (with central 50 or 500 µm crack) and typical boundary condition applied on 2d model (right).

4. Results

Calculations and results received from 3D model described above show a very good agreement with those obtained by Huang. The droplet geometry disintegration presented in Fig.6 corresponds with the spherical droplet in [13] and [18]. There is no significant difference between these two models (3D and 2D). Fig.6 and Fig.7 show a huge pressure increase during a few initial microseconds following by the pressure declension to static pressure connected with a droplet spilling. In time interval after 10 µs there is no considerable pressure value and the droplet is totally disintegrated and starts to form a water film on the rigid surface. The maximum almost of 300 MPa occurs, as predicted, on droplet surface axis of symmetry, while the pressure peaks (Fig.7) decrease in the outwards direction.

2D model containing the scale layer and the steel body in addition focus on the computation of stresses within both, scale layer and steel body. A boundary line between these two materials and place where a crack is located was also deeply studied. The knowledge of the shear stress in such potentially "dangerous" places could give us information about the descaling process mechanism. Fig. 9 presents a typical XY-Stress field, asymmetric along the central axis. The left-hand side of the sample is exposed to negative stress, while the right-hand side is strained positively. Maximum or minimum stress reached ± 450 MPa within 1-2 µs, while the axis of symmetry was free of stress. The graphs in Fig.12 show XY-Stress in several points along the scale-steel boundary line. Significant stress curve differences within the frontier can cause the shearing and the scale layer snapping.

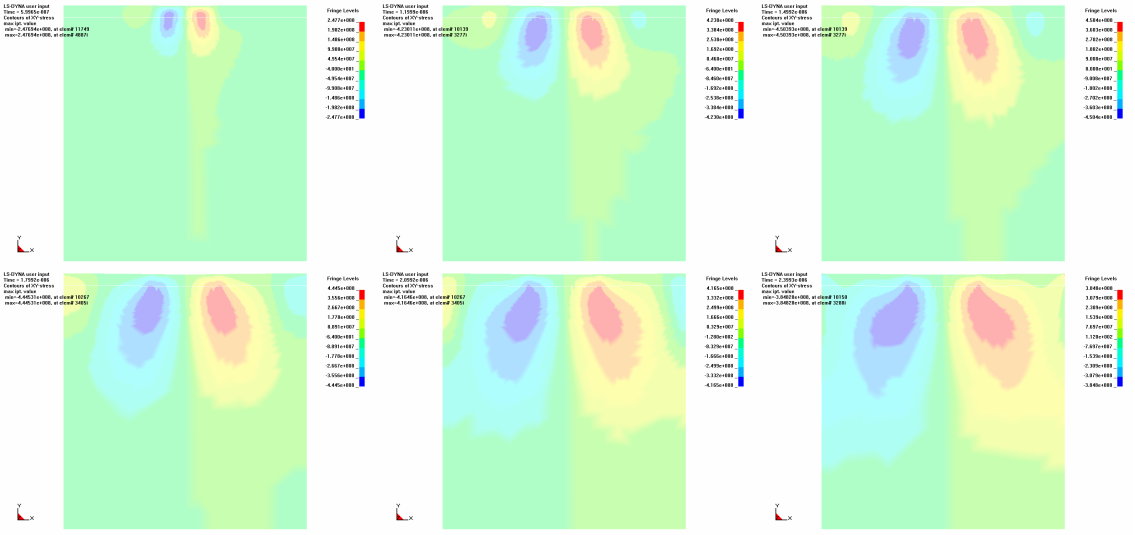

Fig.9: XY-Stress in time interval 0 – 2.5 µs; 500 µm scale layer sample, no crack.

Von Mises Stress field shown in Fig.10 documents a typical time progress during the droplet impact loading. The point of maximum v-m stress continually transfers from the place near by the scale surface deeper to the steel body and area affected by v-m stress propagates symmetrically in all direction. In time interval 1.5 µs v-m stress enhances the maximum value of 1 045 MPa within the steel body. The graphs in Fig.11 show v-m stress along the axis of symmetry. Almost identical maxima on the scale surface and within the steel body are observed, while scale-steel boundary shows the oscillation on a lower level.

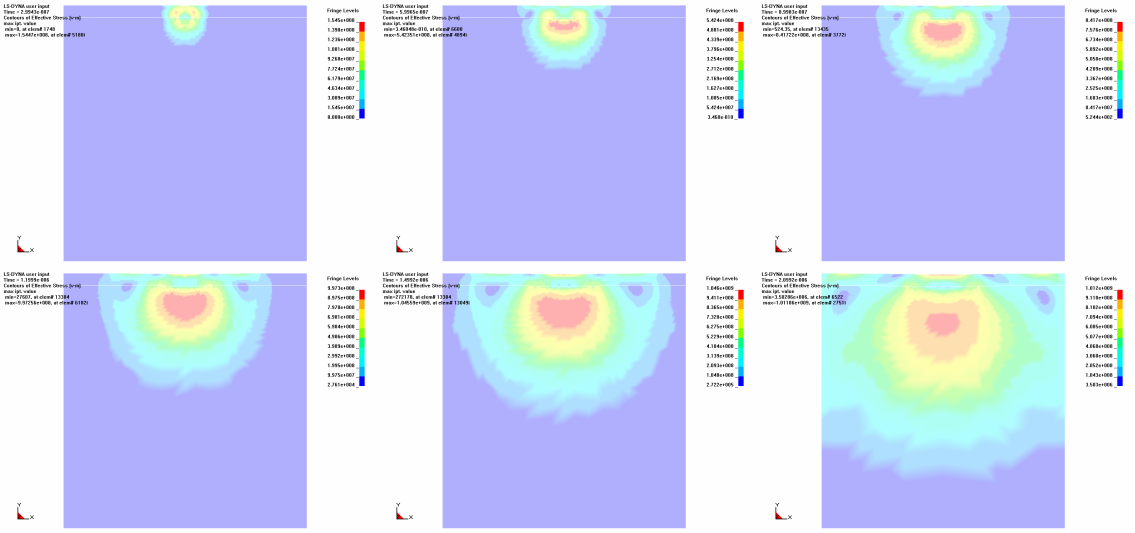

Fig.10: Von Mises Stress in time interval 0 – 2.5 µs; 500 µm scale layer sample, no crack.

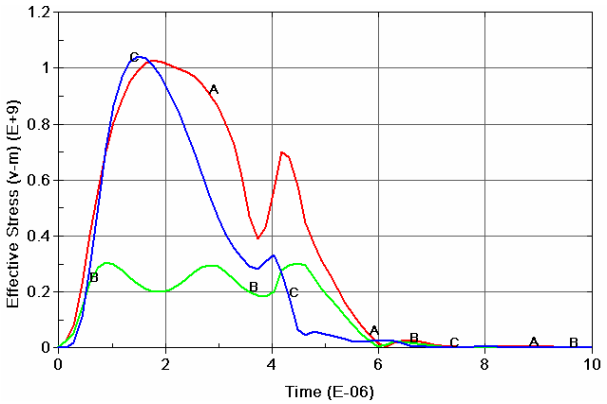

Fig.11: Von Mises Stress history along axis of symmetry; red line (A) scale surface, green (B) scale-steel boundary line and blue (C) within steel body; 500 µm scale layer sample, no crack.

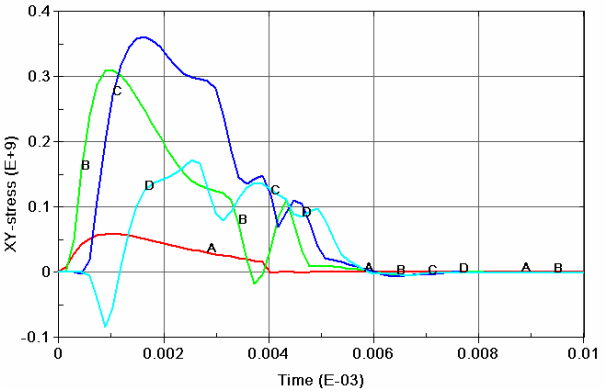

Fig. 12: XY Stress history along boundary line; red line (A) axis of symmetry, green (B) 0.5 mm, blue (C) 1 mm and cyan (D) 1.5 mm from axis of symmetry; 500 µm scale layer, no crack.

Considering the fact of the very heterogeneous scale structure full of micro-cracks realistic modelling of this phase is very difficult. The important thing to know is how these dislocations change the stress distribution within steel-scale composition. Figs. 13 and 14 compare the time stress histories in the area close to the model crack. The differences between the models with and without crack must be taken in account. Inserting of crack to the model cause increase of stresses maximum (10-times higher v-m stress and 20 times higher for x-y stress) and the changes in stress curve shape (v-m stress oscillation for a non-crack case and opposite x-y stress loading).

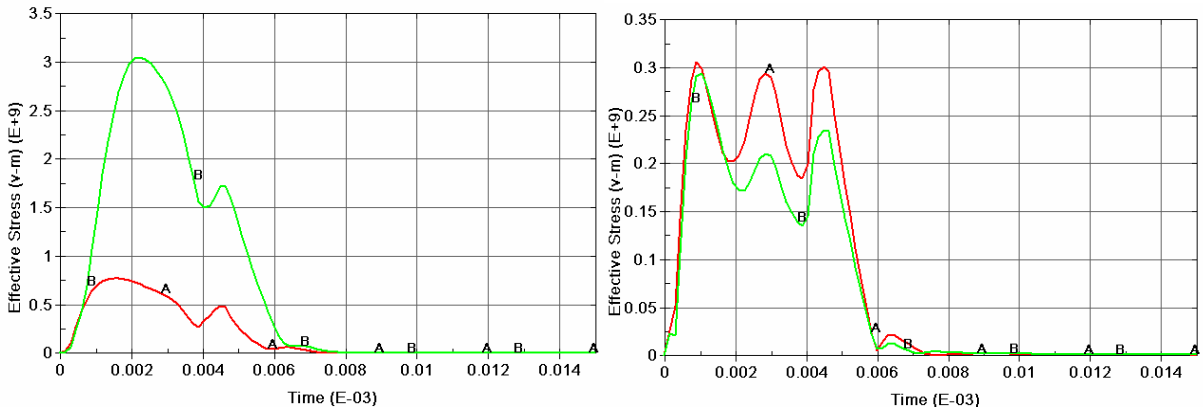

Fig.13: Von Mises Stress history in place of crack; red line (A) scales surface and green (B) steel surface; left sample with central crack and right sample with no crack (C); 500 µm scale layer.

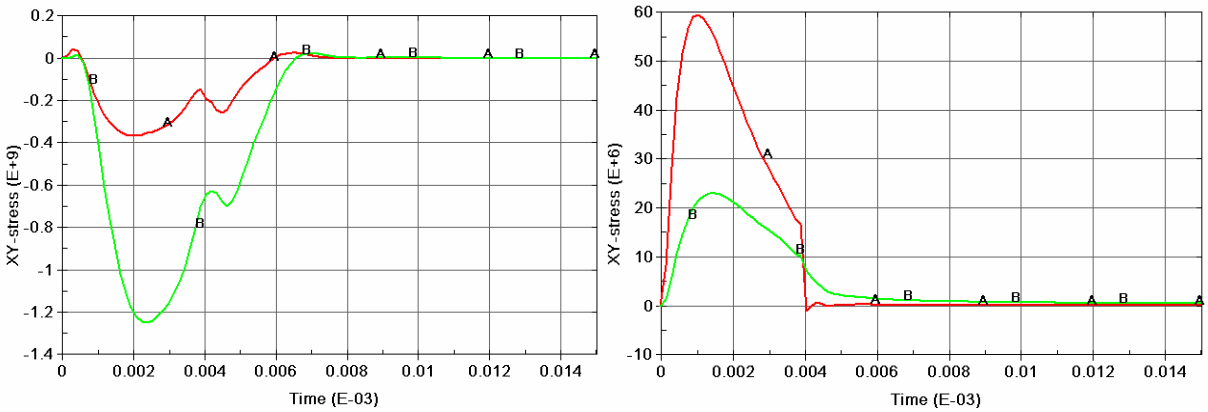

Fig.14: XY Stress history in place of crack; red line (A) scales surface and green (B) steel surface; left sample with central crack and right sample with no crack (C); 500 µm scale layer.

5. Conclusions

The models presented in this paper confirm the hypothesis of the extremely high and very fast impact pressure caused by the high-speed single water droplets. This pressure is transferred into the impacting material (in this case of steel-scale composition) and is transformed to extremely high stress within the sample. Scale surface during descaling process is loaded not only by the single drop, but by the whole water jet flowing from the nozzle atomized into a very high number of drops of different diameters and velocities. Usually, some mean diameter and impact velocity can be determined, but total loading is very random and full of pressure shock waves. Actually as shown in Fig.4 the droplet geometry cannot be easily described, but still the impact pressure is in order of hundreds of MPa and duration in µs (Fig.7).

There are at least two proofs that the high pressure peaks really occur. The first one is an in-direct but easily repeatable test. If a piezoelectric pressure sensor with the maximum allowed the pressure of 20 MPa for the measurement pressure in impact area of a descaling nozzle where pressure of 2 MPa is expected then it will be destroyed by overloading soon. The second test can be done with the samples of the material with different strengths. Jet from the descaling nozzle with impact pressure of 2 MPa can easily make cutting in materials such as aluminum, brass and even steel during several minutes. This would not be possible if there is a pressure not exciting 2 MPa. Huge differences between the measured and real impact pressure are due to the size of the pressure sensor. The non-zero size sensors (Fig.2) provide lower and wider pressure maximum.

The droplet impact creates mostly XY and Von Mises stress. Such a loading is very similar to the rail loading made by wheel known as the Hertz pressure. XY stress is axially symmetric with the maximum ± 450 MPa within 1-2 µs, while Von Mises Stress takes the maximum value of 1 045 MPa in the central part of the model. These intensive stresses may play an important role during the scale snapping. A very important role plays the scale morphology, e.g. in the place of the crack v-m stress is 10 times and xy-stress is even 20 times higher. On the other hand the scale thickness influences only xy stress (50% fall), but v-m stress remains

almost constant. A weak point of this model can be an assumption of homogenous properties of scales, because their random structure cannot be properly modeled.

The study confirms that high velocity of the water droplet has due to the water-hammer effect sufficient kinetic energy to break the scale layer and can be considered as one of mechanisms explaining descaling processes. The real state must be the combination of mechanical, thermal and vapour explosion approaches. The question is how significant are these descaling theories in the light of new observations.

6. Acknowledgment

This investigation was financially supported by the Czech Grant Agency, No. 106/06/0709.

7. References

1. Blazevic, "Newton and descaling", 3rd conf. Hydraulic Descaling, London 2000.
2. Bendig, Raudensky and Horsky, "Descaling with High Pressure nozzles", ILASS-Europe, Zurich, 2001.
3. Raudensky, Horsky, Pohanka, Tosovsky and Kotrbacek, "Experimental Study of Parameters influencing Efficiency of Hydraulic Descaling – Theory of Vapor Explosion", 4th Conference on Hydraulic Descaling, London, 2003, pp. 29-40.
4. Foldyna, J. et al., "Utilization of ultrasound to enhance high-speed water jet effects", Ultrasonics Sonochemistry, 11 (2004), 131-137.
5. Foldyna, J., "Rozpojování hornin vysokorychlostními pulzními paprsky", PhD thesis, Ostrava.
6. Smith, D.G. and Kinslow, R., "Pressure Due to High-velocity Impact of a Water Jet", Experimental Mechanics, January1976.
7. Huang, Y.C., Hammit, F.G. and Mitchell, T.M., "Note on shock-wave velocity in high-speed liquid-solid impact", Journal of Applied Physics, Vol. 44, No. 4, April 1973.
8. Heyman, F.J., Journal of Basic Engineering 90, 400 (1968).
9. Heyman, F.J., "High-speed Impact between a Liquid Drop and a Solid Surface", Journal of Applied Physics, Vol. 40, No. 13, December 1969.
10. Bruton, J.H., "Deformation of Solids by Impact of Liquids at High Speeds", Symposium on Erosion and Cavitation, 1961.
11. Beckman, G., Krzyzanonowski, J.A., "New Model of Droplet Impact Wear", Proc. 7th Int. Conf. on Erosion by Liquid and Solid Impact.
12. Hammit, F.G. et al., "Experimental and Theoretical Research on Liquid Droplet Impact", 319-345.
13. Huang, Y.C., Hammit F.G., "Numerical Studies of Unsteady, Two-Dimensional Liquid Impact Phenomena", Report No. UMICH 03371-8-T, July 1971.
14. Huang, Y.C., Hammit F.G., "Liquid Impact on Elastic Solid Surface", Report No. UMICH 03371-8-T, July 1971.
15. Huang, Y.C. et al., "Normal Impact of a Finite Cylindrical Liquid Jet on a Flat Rigid Plane", Report No. UMICH 03371-9-T, August 1971.
16. Huang, Y.C. et al., "Spherical Droplet Impingement on Flat Rigid Surface Non-Slip Boundary Conditions", Report No. UMICH 03371-14-T.
17. Huang, Y.C. et al., "Hydraulic Phenomena During High-Speed Collision Between Liquid and Rigid Plane", Journal of Fluids Engineering, June 1973, 276-294.

18. Huang, Y.C. et al., “Mathematical modelling of normal impact between a finite cylindrical liquid jet and non-slip, flat rigid surface”, first international symposium on jet cutting technology, April 1972, Coventry, A4 57-68.
19. Lesser, M.B., Field, J.E., “The fluid mechanics of compressible liquid impact”, Proc. 4th Int. Conf. on Rain Erosion and Associated Phenomena, 1974, Meersburg, 235-269.
20. Niesytto, J., Niesytto, J.T., “Collision of liquid drop with an elastic halfspace”, Proc. 7th Int. Conf. on Erosion by Liquid and Solid Impact.
21. Tošovský, J.,“Stress Analysis of Scale Layer for Descaling Process“.